Preliminary coating design and coating developments for ATHENA

Anders C. Jakobsen[a], Desiree Della Monica Ferreira[a], Finn E. Christensen[a], Brian Shortt[b], Max Collon[c], Marcelo D. Ackermann[c]

[a]DTU Space, Juliane Maries Vej 30, 2100 Copenhagen Ø, Denmark);
[b]European Space Research and Technology Ctr. (Amsterdam, Netherlands)
[c]Cosine Research B.V. (Leiden, Netherlands)

ABSTRACT

We present initial novel coating design for ATHENA. We make use of both simple bilayer coatings of Ir and B_4C and more complex constant period multilayer coatings to enhance the effective area and cover the energy range from 0.1 to 10 keV. We also present the coating technology used for these designs and present test results from coatings.

1. INTRODUCTION

In this paper we investigate the possibility of increasing the ATHENA telescope effective area in the range between 0.1 and 10 keV. We studied the performance of five different material combinations, W/Si, Ir/B_4C, Pt/C, Pt/B_4C and Mo/Si, considering a simple bilayer, simple multilayers and linear graded multilayers. To reduce stress in the Ir/B4C coating, we investigated the need of a third stress reducing material as an undercoat to the Ir/B4C bi-layer.

The ATHENA mission consists of two identical telescopes with fixed focal planes, the first containing a calorimeter spectrometer and the second a wide field imager. The ATHENA focal plane is of 11.5 m, the telescopes innermost radius of 0.15 m and outermost radius of 0.90 m. The operational energy range is from 0.1 to 10 keV.

The coating recipe adopted as baseline is a bilayer with an 8 nm layer of B_4C on top of a 10 nm Ir layer. The same coating is adopted for all mirror modules at all radii.

2. OPTIMIZING ATHENA COATING DESIGN - PRELIMINARY RESULTS

2.1 Low energy range

The choice for radii division and coating recipes is based on the need of optimization at different energy ranges. The use of a simple bilayer coating is appropriate for energies lower than 5 keV, while to improve the telescope performance above 5 keV the use of multilayers is required.

The telescope radius where simple bi-layers should be applied is considered to be the radius at which the reflectance of the Ir/B_4C baseline coating at 6 keV is above 30%. This is a somewhat arbitrary choice and considered as a good starting point for investigation. This radius corresponds to the seven innermost rows of mirror modules, see figure 1. The optimization of bi-layer coating is performed for this region (radius between 0.15 m to 0.59 m).

The criterion applied for the choice of a simple bilayer coating material is based on the coating performance at 1 keV and 6 keV considering the seven innermost rows of mirror modules.

We computed the best coating thickness for each material combination in order to maximize the effective area at 1 keV and 6 keV. The surface roughness considered is 0.65 nm for Ir/B_4C, and 0.45 nm for W/Si, Pt/C,

Further author information: (Send correspondence to A.C.J.)
A.C.J.: E-mail: jakobsen@space.dtu.dk, Telephone: +45 3532 5735
D.D.M.F.: E-mail: desiree@space.dtu.dk, Telephone: +45 3532 5734

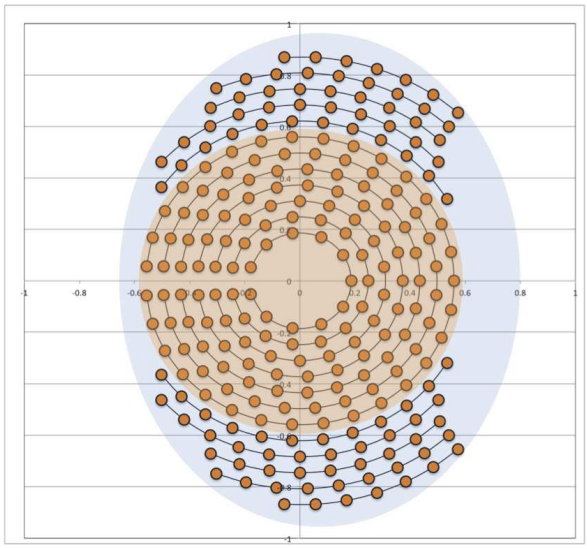

Figure 1. Diagram of one of two telescope optics for ATHENA. Each orange circle represents a mirror module with 68 coated SPO substrates. The inner part chosen for simple bilayer/trilayer and outer part chosen to carry a multilayer with cap layer and top layer.

Pt/B_4C and Mo/Si. We observe that Pt/B_4C presents superior effective areas at both energies, followed by Ir/B_4C.

Because the material combination of Pt/B_4C is still unknown at the present time, and properties such as roughness and stress need further investigation, Ir/B_4C is considered as the best option for a bi-layer coating.

We investigate the best layer thickness to maximize the on-axis effective area at 6 keV considering a Ir/B_4C coating. As the effective area scales with the reflectivity square, we base our study on the reflectivity curve computed at this energy. To optimize the Ir/B_4C coating we vary the thicknesses of Ir and B_4C and compute the on-axis effective area at 1 keV and at 6 keV. We list the parameter combinations that provide maximum effective area at those energies and parameter combinations resulting in 99% and 95% of the maximum effective area. The best parameter combination provides minimal loss of on-axis effective area on both energies. Based on the on-axis effective areas at 1 keV and 6 keV and on the layer thickness we find that the baseline (10 nm Ir, 8 nm B_4C) is the optimum choice.

2.2 Mid energy range

At radii beyond the seven innermost mirror module rows (0.59 m) the bi-layer reflectivity is inefficient at energies above 6 keV. To enhance the telescope effective area at the energy range from 5 to 10 keV, we suggest a multilayer coating approach for the 5 outermost mirror module rows.

Also here the material choice is defined by evaluating the on-axis effective area at 6 keV for this region (0.59 0.90 m). We consider a simple multilayer coating for the same materials listed above, a cap layer of the heaviest material and an 8 nm overcoat of B_4C to account for the energies below 1.5 keV. The surface roughness applied is 0.65 nm for Ir/B_4C and 0.45 nm for the remaining material combinations.

The parameters considered in the computation are: number of bi-layers, thickness of the bi-layers, ratio between heavy and light material thickness and thickness of the extra layer of the heavy material. The best parameters for each material choice return maximum on-axis effective area at 6 keV.

Applying a multilayer of W/Si results in the best performance considering the criterion above with the second best options being Pt/B_4C and Pt/C with equivalent performances. The material combinations Pt/B_4C and Pt/C return on-axis effective areas that differ from the computed for W/Si by only 2%. There are several reasons for choosing Pt over W, e.g. the absorption edges around 1-2 keV, and those aspects are under investigation. At this point we proceed with the optimization of the telescope outermost rows considering W/Si as the best material choice for multilayer coating.

2.3 Multilayer optimization

The actual ATHENA coating baseline presents optimal performance at energies below 5 keV but the use of multilayers in the outer mirror module rows can increase the telescope effective area at energy range 5 to 10 keV. The optimum coating design so far is a bi-layer of Ir/B_4C with thickness of 10 nm and 8 nm respectively, applied to the seven innermost mirror module rows. The remaining five outermost rows are optimized considering multilayers of W/Si with a W cap layer and an 8 nm B_4C overcoat.

To optimize the coating design at the telescope outermost region we considered five different coating recipes, one for each row. The motivation for this choice is the need of a smooth effective area curve at the scientifically interesting region around 6 keV.

A linear graded multilayer is chosen over a simple multilayer in order to optimize a wider energy range. The design for optimization is therefore a linear graded W/Si multilayer with a W cap layer on top of the multilayer and an 8 nm B_4C overcoat. The B_4C overcoat is optimized for best performance at 1 keV and is therefore set to 8 nm.

For each row in the region between 0.59 m and 0.90 m an optimal coating recipe is computed in order to maximize the effective area in the region around 6 keV without compromising the effective area at lower energies. This is achieved by evaluating the several possible parameter combinations that result in the maximum integrated effective area over energy for the energy range between 3 keV and 8 keV with the condition that the loss of effective area between 1.5 and 5 keV is minimal. To achieve that we look at how the gradient of the on-axis effective area changes over the energy range between 3 keV and 8 keV and look for solutions returning maximum effective area with minimum gradient, i.e. the curve should be as flat as possible. This approach is preliminary and alternative choices for the figure of merit are being investigated.

The parameters considered in this computation are: Number of W/Si bi-layers (n), thickness ratio between W and Si (Si-Γ), minimum bi-layer thickness (d_{min}), maximum bi layer thickness (d_{max}) and thickness of the W cap layer (d_W) (to accommodate the energies between 1.5 keV and 5 keV). The parameters were varied considering steps of 10 bilayers, 0.1 for Si-Γ, 0.5 nm for d_{min} and d_{max} and 1 nm for d_W.

The best parameters for each row are listed in table 1. The optimized effective area over energy is shown in figure 2. The comparison between the baseline performance at 1 keV and 6 keV is shown in table 2.

Row	n	Si-Γ	d_{min} [nm]	d_{max} [nm]	d_W [nm]
8	10	0.5	5.5	7.5	8.0
9	10	0.5	5.0	7.5	8.0
10	20	0.6	4.0	7.0	7.0
11	30	0.7	3.5	6.5	6.0
12	20	0.6	4.0	6.5	6.0

Table 1. Optimized coating design for the outermost mirror module rows of ATHENA assuming a linear graded multilayer

	Baseline	Optimized
A_{eff} at 1 keV [m^2]	1.146	1.152 (+0.4 %)
A_{eff} at 6 keV [m^2]	0.431	0.454 (+5.6 %)

Table 2. Effective area of ATHENA. Results listed for 2 telescopes with a 10% reduction applied to account for eventual losses due to e.g. alignment and particle contaminations.

3. SILICON PORE OPTIC SUBSTRATES

The optics of ATHENA will consist of >60,000 Silicon Pore Optic (SPO) mirror substrates.[1] Each substrate is cut from a wafer in sizes of 66 mm x 66 mm and have grooves cut into the bottom side so the substrate gets thin ribs, which gives the substrates the ability to be stacked directly on top of each other. The top surface of the substrate is treated with a SiO_2 wedge with a specific slope so each SPO substrate has the right angle to the focal plane.

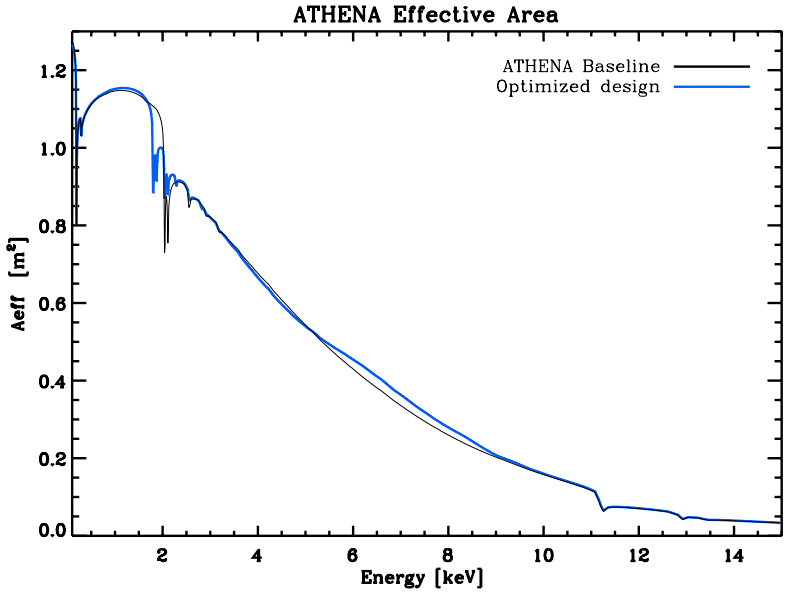

Figure 2. ATHENA optimized design and baseline. Results listed for 2 telescopes with a 10% reduction applied to account for eventual losses due to e.g. alignment and particle contaminations.

The stacked plates are bonded using direct Si-Si contact, which requires part of the surface of every substrate to be free of coating so the ribs can have direct contact to the Si wafer surface. During DC Magnetron sputtering the entire surface is coated, unless a mask is used during coating to shield part of the substrate from incoming sputtered atoms. This has previously been investigated, but the alignment of a mask for every substrate is a very cumbersome task, especially for more than 60,000 substrates.

Another solution is to use a striped resist layer, which can be removed along with any film deposited on top after coating. An example of that can be seen in figure 3, where a Ir/B_4C bilayer is deposited on a SPO substrate with a resist layer. The resist along with film is removed after coating using acetone and results in a substrate with bare Si-substrate stripes so another SPO substrate can be stacked on top.

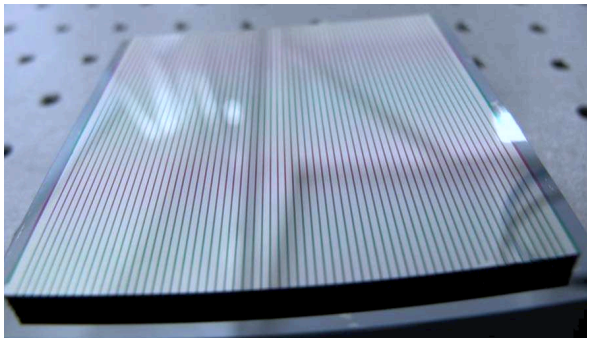

Figure 3. A coated Silicon Pore optic substrate with coating removed in a striped pattern using a resist layer.

To achieve a clean separation of coated film from the substrate in the specified striped pattern, the sputter deposited thin film needs a good adhesion to the areas of the substrate without resist layer. One factor that can be connected to bad adhesion is stress in the thin film, and the Ir/B_4C bilayer films have a compressive stress of >4 GPa during preliminary coating tests at DTU Space.

4. REDUCING STRESS IN IRIDIUM / BORON CARBIDE BILAYERS

To reduce the stress in Ir films, we use of Cr as an underlayer between substrate and Ir. It can decrease and even remove the film stress completely. The addition of a B_4C toplayer complicates the interaction, as sputtered

B_4C films are stressed.

Investigations into the stress reducing ability of Cr on Ir/B_4C bilayers are done, with a further emphasis on the possible change in surface roughness when a Cr underlayer is introduced.

5. EXPERIMENTAL

Sample substrates were coated at DTU Space using a DC Magnetron sputtering chamber.[2] The substrates were mounted in the chamber between two 50 mm deep separator plates with a distance of 100 mm (see figure 4). The separator plates reduce roughness by collimating incoming sputtered atoms, so the amount of sputter atoms coming at a low angle to the substrate surface is decreased.

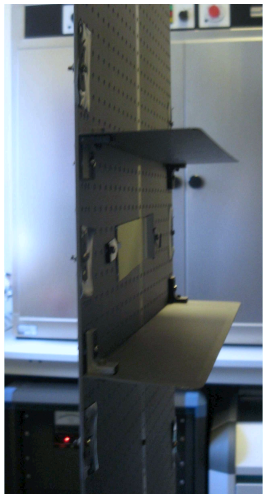

Figure 4. Side view of a mounting plate in the sputtering chamber. A Si wafer substrate is mounted in the middle between two seperator plates.

Each specific film is coated on both a 20x80 mm Si wafer piece with a surface roughness of $\sigma_{\mathsf{rms}} = 0.25$ nm for X-ray reflectometry measurements and a 5x70 mm Si wafer piece for stress measurements. All large Si wafer pieces are measured with a 8 keV Cu-K_α rotating anode at DTU Space and the data is fitted using IMD[3] to determine the geometry of the coated film. The smaller Si wafer pieces were measured before and after coating using a Dektak 150 stylus measurement device, that measures the deflection of a sample and calculates the stress of a coating based on film thickness and difference in deflection before and after coating.

Two sample sets were created, each with eight different coatings as seen in table 3.

Sample	1	2	3	4	5	6	7	8	9	10	11	12	13	14	15	16
d_{Ir} [nm]	∼7	∼7	∼7	∼7	∼7	∼7	∼7	∼7	∼7	∼7	∼7	∼7	∼7	∼7	∼7	∼7
$d_{\mathsf{B_4C}}$ [nm]	∼7	∼7	∼7	∼7	∼7	∼7	∼7	∼7	∼3.5	∼3.5	∼3.5	∼3.5	∼3.5	∼3.5	∼3.5	∼3.5

Table 3. Overview of samples coated with Ir and B_4C.

6. DEVELOPMENT RESULTS

Figure 5 presents results from stylus point deflection measurements, with the left plot showing the change in stress with changing Cr thickness for $d_{\mathsf{Ir}} \approx d_{\mathsf{B_4C}} \approx 7$ nm. The right plot shows the change in stress with changing Cr thickness for bilayer films with $d_{\mathsf{Ir}} \approx 7$ nm and $d_{\mathsf{B_4C}} \approx 3.5$ nm. Each sample are represented as two dots, as both a compressive and tensile stress can be present in the film at the same time.

In both plots a clear change in stress from compressive to tensile is seen as the Cr underlayer thickness is increased.

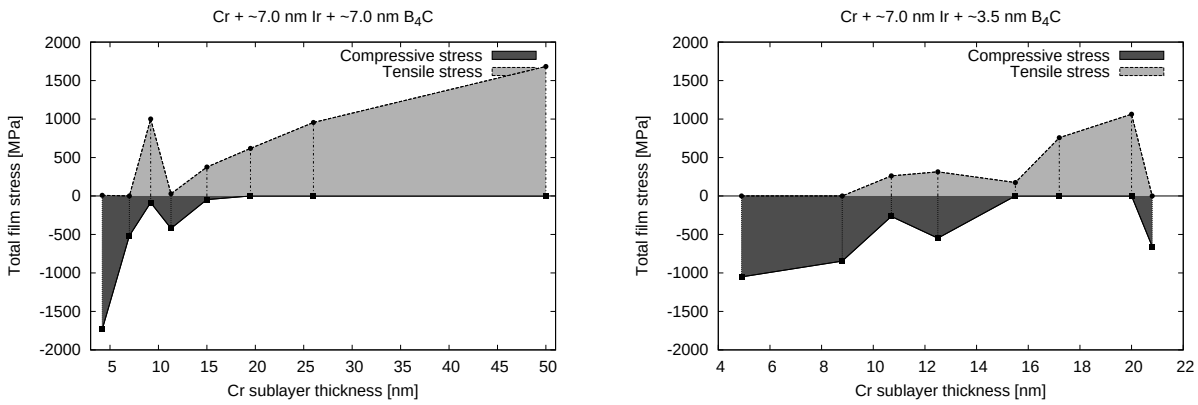

Figure 5. Plots comparing Cr thickness in a trilayer coating with the resulting total film stress. Left side compares Cr/Ir/B_4C coatings with $d_{Ir} \approx d_{B_4C} \approx 7$ nm. Right side compares Cr/Ir/B_4C coatings with $d_{Ir} \approx 7$ nm and $d_{B_4C} \approx 3.5$ nm.

The change in stress correlates with earlier investigations of Ir coatings with Cr underlayer. The stress decreases with increasing Cr thickness and the film eventually comes close to zero stress. Adding even thicker layers of Cr underneath will yield a tensile stress in the film. For Ir/B_4C bilayers of these dimensions, the film stress can be reduced to ~ 0 using a Cr underlayer with a thickness of $\sim$7 nm to $\sim$11 nm.

The data points for the left plot in figure 5 show a consistent curve going from compressive to tensile stress, except around the intersection point with 0 stress. Two samples show values outside the expected and outside standard error deviation. Further investigation in the low stress region is planned.

The right side plot in figure 5 shows several deviations from the expected values, but still a correlation can be seen. The intersection point with 0 stress is with Cr thickness of 12 to 14 nm. The decreased thickness of the B_4C layer has shown a considerable alteration of the structural properties of the film and thus requires a thicker Cr underlayer to minimize the total film stress.

Figure 6 shows X-ray reflectometry data from two different large Si wafer samples and the data is fitted using IMD. The left plot shows data from a trilayer of Cr/Ir/B_4C with relative thicknesses of 11 nm/7 nm/7 nm, the right plot shows data from a Cr/Ir/B_4C trilayer with relative thicknesses 4 nm/7 nm/3.5 nm.

The fit shows a surface roughness of Ir in the left plot of $\sigma_{\mathsf{rms}} = 0.5$ nm and for Cr $\sigma_{\mathsf{rms}} = 0.7$ nm. The surface roughness of B_4C does not affect 8 keV photons significantly in IMD simulations, so a precise value of the roughness can not be given using this measurement method. In these fits, the B_4C roughness is set to $\sigma_{\mathsf{rms}} = 0.4$ nm. In the right plot, Ir surface roughness is significantly smaller ($\sigma_{\mathsf{rms}} = 0.2$ nm) and so is the Cr surface roughness ($\sigma_{\mathsf{rms}} = 0.5$ nm).

The change in Ir roughness was expected when changing the Cr thickness. Sputtered Cr films generally have a rough surface, and the roughness increases with thicker layers. That the Ir surfaces are smoother than the Cr surfaces were not expected, as the expected lower bound for film surface roughness is the surface roughness on which the film is coated. So e.g. an Ir layer coated onto a Cr surface with roughness of 0.7 nm would also give an Ir surface roughness of at least 0.7 nm. Since this is not the case in either of the two samples, the Ir and Cr combination can be suspected to give a smoothening effect on above surfaces.

For the right side plot in figure 6, the Ir surface roughness is even lower than the Si wafer substrate surface roughness (0.25 nm). This smoothening effect could be present in Cr + Ir coatings on rougher substrates, which begs for further investigation.

As the coatings done here are deposited onto normal Si wafer substrates and not wedged SPO substrates, XRR measurements of the bare substrates were done. The measurement data can be seen in figure 7 along with fits modelled using IMD.

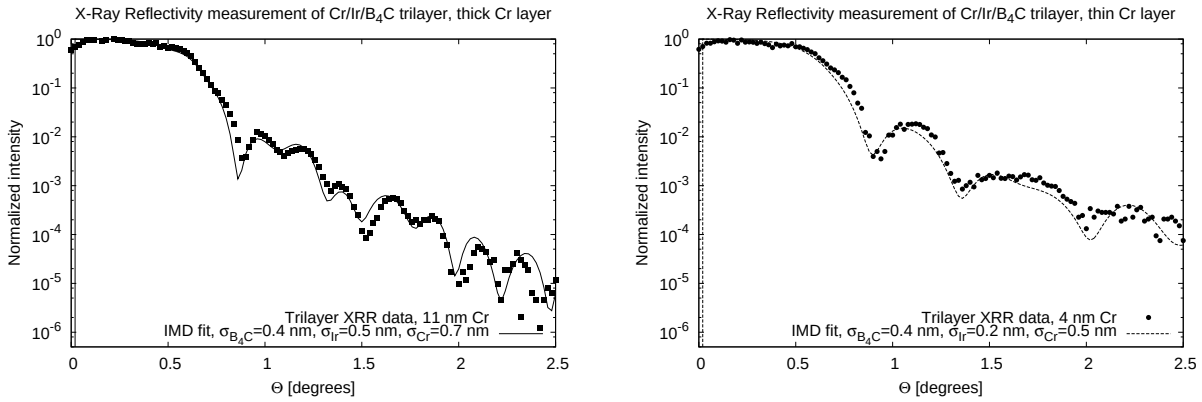

Figure 6. Plots showing X-ray reflectometry data for two different trilayer coated samples. Each data set is fitted a model from IMD to get film dimensions and surface/interface roughness values. The left side shows data from a trilayer of $Cr/Ir/B_4C$ with relative thicknesses of 11 nm/7 nm/7 nm, the right side shows data from a $Cr/Ir/B_4C$ trilayer with relative thicknesses 4 nm/7 nm/3.5 nm.

In the left plot is shown measurement data of a bare Si wafer substrate, and the IMD model fits to the data with a substrate surface roughness of $\sigma_{\mathsf{rms}} = 0.25$ nm. The plot on the right shows the measurement data for a wedged SPO substrate. The IMD model fits to the data with a substrate roughness of $\sigma_{\mathsf{rms}} = 0.45$ nm.

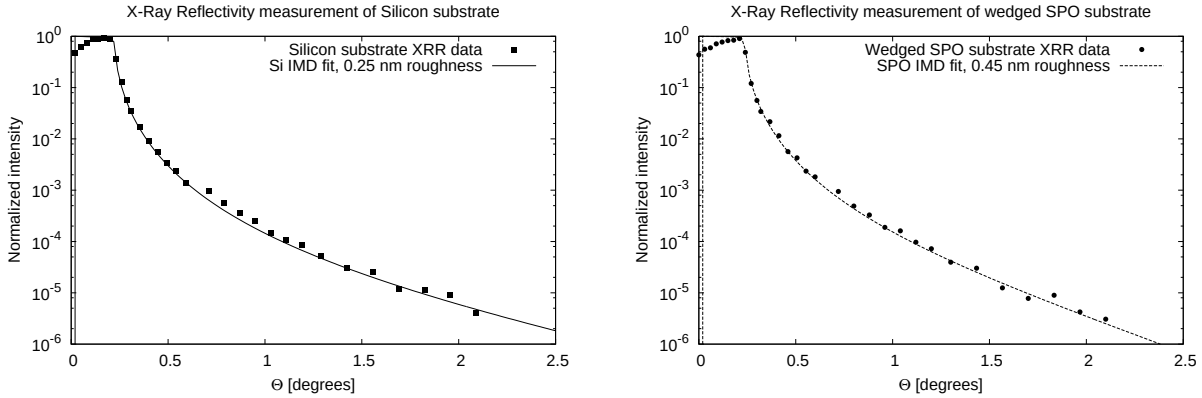

Figure 7. Plots showing X-ray reflectometry data for a bare Si wafer substrate (left side) and a wedged SPO substrate (right side). Each data set is fitted using an IMD model to get surface roughness values.

The increased roughness of wedged SPO substrates compared to bare Si wafer substrates were taken into account during the optimization procedure in section 2.1 where all surface roughness values were expected to be at least 0.45 nm.

The SiO_2 material of the wedge on the SPO substrate might yield different sputtered film properties due to different interatomic spacing in the amorphous surface. All possible coating candidates will be tested on proper wedged substrates in the next months.

7. CONCLUSION

A preliminary coating design optimization of the ATHENA optic has been shown, using an analytical approach to achieve optimum coating recipes for the outer five mirror module rows. The optimized coating uses linearly graded multilayers to increase the effective area around 6 keV by ~ 5 %.

Additionally, trilayer coatings of $Cr/Ir/B_4C$ were deposited onto Si wafer substrates to investigate film stress and surface roughness properties. A correlation between Cr thickness and film stress has been found, where a Cr

underlayer can remove most of the stress in a Ir/B_4C film. A thicker Cr underlayer to reduce stress is necessary when decreasing the B_4C layer thickness in a Ir/B_4C bilayer. Finally, XRR measurements have shown that although Cr surface is relatively high, the surface roughness of Ir layers deposited on top of Cr were consistently lower.

8. FUTURE INVESTIGATIONS

Results on coating design for ATHENA presented here are preliminary. Several aspects of the coating design optimization are undergoing further investigation and improvement. Other material combinations will be investigated as well as the possibility of changing the amount of mirror modules coated with trilayer vs. multilayers.

Work to be done in coating development includes the introduction of reactive sputtering using N_2 gas[4,5] to reduce film stress and surface/interface roughness as well as using honeycomb collimation[6] during sputtering. Film stress in multilayers and the removal of stress using Cr underlayers will also be investigated. X-ray reflectometry and X-ray scattering will be performed at BESSY. Additional measurement techniques will be used, such as cross-sectional TEM, Atomic Force Microscopy and X-ray fluorescence.

REFERENCES

[1] Wallace, K., Bavdaz, M., and Gondoin, P., "Silicon pore optics development," *Proceedings of SPIE* **7437**.

[2] Jensen, C., Christensen, F., Chen, H., Smitt, E., and et al, "Multilayer coating facility for the HEFT hard x-ray telescope," *Proceedings of SPIE* **4496**, 104–108 (Jan. 2002).

[3] Windt, D., "IMD—Software for modeling the optical properties of multilayer films," *Computers in Physics* **12**, 360–370 (Jan. 1998).

[4] Windt, D., "Reduction of stress and roughness by reactive sputtering in W/B4C X-ray multilayer films," *Proceedings of SPIE* **6688** (Jan. 2007).

[5] Bellotti, J. and Windt, D., "Depth-graded Co/C multilayers prepared by reactive sputtering," *Proceedings of SPIE* **7437** (Jan. 2009).

[6] Anette, V. and Carsten, P., "Collimated Magnetron Sputter Deposition for Mirror Coatings," *X-Ray Optics and Instrumentation* **2008** (Jan. 2008).